Journal of the European Ceramic Society 5 (1989) 113–122

Sintering of Amorphous Polymer-Derived Si, N and C Containing Composite Powders

Ralf Riedel

Max-Planck-Institut fur Metallforschung, Institut fur Werkstoffwissenschaft, Pulvermetallurgisches Laboratorium, D-7000 Stuttgart 80, FRG

Martin Seher & Gerd Becker

Institut fur Anorganische Chemie der Universitat Stuttgart, D-7000 Stuttgart 80, FRG

(Revised version received 27 July 1989, accepted 31 July 1989)

Abstract

In the present work a Si_3N_4 composite containing 24 wt% SiC particulates was prepared by sintering a polysilazane-derived amorphous Si–N–C powder Al_2O_3 and Y_2O_3 were added as sintering additives The amorphous powder was pressureless sintered to 97% relative density at 1750°C in nitrogen atmosphere α-Si_3N_4 and β-SiC were generated in situ *due to the crystallization of the amorphous powder during the heating in the densification process Subsequently, α-Si_3N_4 is transformed to the β-form by the liquid phase sintering mechanism A fine-grained microstructure ($d_{50} = 0.2\,\mu m$) with the SiC particulates homogeneously distributed in the Si_3N_4-matrix was found in the densified samples Room temperature fracture strength (σ_B) and fracture toughness (K_{Ic}) were similar to those measured in conventionally processed composites However, the fracture strength was characterized by a relatively low standard deviation indicative of the better reproducibility of the properties due to improved homogeneity in the developed microstructure*

Die vorliegende Arbeit berichtet uber die Herstellung einer Si_3N_4/SiC Verbundkeramik (24 Masse% SiC), ausgehend von amorphem Si–N–C-Pulver Die Synthese des Komposit-Pulvers erfolgte durch Pyrolyse eines Polymethylsilazans Al_2O_3 und Y_2O_3 wurden als Sinteradditive zugesetzt Das amorphe Pulver konnte drucklos bei 1750°C in einer Stickstoffatmosphare bis zu 97% relativer Dichte gesintert werden Aufgrund der Kristallisation, die wahrend des Aufheizens im Verdichtungsprozeß einsetzt, werden zunachst α-Si_3N_4 und β-SiC gebildet Anschließend wird α-Si_3N_4 durch das ablaufende Flussigphasensintern in β-Si_3N_4 umgewandelt Das Sintergefuge ist extrem feinkornig ($d_{50} = 0.2\,\mu m$) und zeichnet sich durch eine homogene Dispersion der SiC-Partikel in der Si_3N_4-Matrix aus Die gemessenen σ_B- und K_{Ic}-Werte sind vergleichbar mit denen konventionell aufbereiteter Si_3N_4/SiC-Verbundwerkstoffe Die Biegebruchfestigkeiten der aus dem Polysilazan hergestellten Komposits zeigen jedoch relativ geringe Standardabweichungen, was auf eine hohere Reproduzierbarkeit der Eigenschaften aufgrund der verbesserten Homogenitat des entwickelten Gefuges hinweist

On a préparé au cours de cette étude un composite de Si_3N_4 contenant 24% massiques de particules de SiC par frittage d'une poudre amorphe de Si–N–C provenant d'un polysilazane Al_2O_3 et Y_2O_3 ont été ajoutés pour permettre le frittage La poudre amorphe atteint une densité relative de 97% par frittage naturel à 1750°C sous azote Du Si_3N_4 α et due SiC β cristallisent in situ *pendant le chauffage de la poudre amorphe lors du processus de densification Le Si_3N_4 α est ensuite transformé en phase β par le mécanisme du frittage en phase liquide Les frittés denses présentent une microstructure fine ($d_{50} = 0.2\,\mu m$) et une distribution homogène des particules de SiC dans la matrice de Si_3N_4. La résistance à la flexion à température ambiante et la ténacité sont similaires à celles mesurées sur des composites produits de façon conventionnelle La résistance à la fracture est*

Journal of the European Ceramic Society 0955-2219/89/$3 50

cependant caractérisée par un écart-type relativement bas, preuve de la meilleure reproductibilité des propriétés en raison de l'homogénéité accrue de la microstructure

1 Introduction

The incorporation of SiC into Si_3N_4-matrices increases their hardness, creep and oxidation resistance compared to pure Si_3N_4 materials [1] However, the fabrication of dense ceramic composite materials is difficult in general, due to the influence of backstresses which can develop during densification from the different sintering behaviour of the individual dispersed phases [2-4] Thus, for example, the preparation of Si_3N_4/SiC composites with high relative densities ($\geq 98\%$) is achieved only by hot- or hot-isostatic-pressing.[5] The addition of oxide sintering aids like Al_2O_3 and Y_2O_3 does allow pressureless sintering of the Si_3N_4/SiC-system up to reasonable densities ($\geq 95\%$ relative density) provided that the SiC content of the mixture does not exceed a certain amount, i e, 17 wt% as has been reported by Greil *et al* [1] Generally, it is found that depending on the viscosity of the liquid phase and on the matrix grain size, greater amounts of SiC lower the sintered matrix density The production of composite materials, where the different phases are homogeneously distributed, requires relatively complex milling procedures applied to the starting powders However, milling is always a source of contamination and the purity as well as the homogeneous distribution of the composite phases, i e. the chemical homogeneity of the powders, is also important for the uniform densification of the green body and for the reproducibility of the mechanical and physical properties of the sintered composite

For these reasons, the aim of the present study has been to improve the homogeneity of SiC dispersed in a Si_3N_4-matrix and to improve the sintering conditions In a recent paper,[6] we have reported the successful preparation of a dense Si_3N_4/SiC composite attained by mixing commercial Si_3N_4-powder with an organometallic SiC precursor Subsequent pyrolysis and sintering of the polymer/powder mixture yielded a fine-grained Si_3N_4 microstructure containing up to 10 wt% of a homogeneously distributed β-SiC phase In a model study, we now investigate the preparation of dense Si_3N_4/SiC composites by the sintering of an amorphous polymer-derived Si, N and C containing composite powder The amorphous state favours the homogeneous distribution of the elements in the starting powder and, hence, the homogeneous in-situ generation of the crystalline composite phases during the sintering process Furthermore, amorphous powders can exhibit a higher sinterability compared with that of crystalline powders [7]

2 Experimental Procedure

The amorphous Si, N and C containing powder was prepared by the pyrolysis of a polymethylsilazane at temperatures up to 1000°C in an argon atmosphere The synthesis, structure and pyrolysis behaviour of the polysilazane, $[CH_3SiHNH]_{0.4}[CH_3SiN]_{0.6}$, has been described elsewhere [8]

The polymethylsilazane was mixed with Al_2O_3 and Y_2O_3 as sintering aids prior to pyrolysis The oxides were added in such amounts that the powder mixture contained 10.5 wt% Al_2O_3 and 4.5 wt% Y_2O_3 after pyrolyzing the polymer-oxide-mixture in an argon atmosphere The processing was conducted as follows in a round-bottom flask, equipped with a side arm with a stop-cock to the argon and vacuum supply, 80 g polymethylsilazane, $[CH_3SiHNH]_{0.4}[CH_3SiN]_{0.6}$, was dissolved in 300 ml tetrahydrofuran (THF) under argon atmosphere After addition of 8.4 g Al_2O_3 (A 16, Alcoa, Pittsburgh, PA, USA) and 3.6 g Y_2O_3 (99.99% purity, Ventron Alfa Produkte, Karlsruhe, FRG), the THF was evaporated in vacuum at 10^{-3} mbar (0.1 Pa) and room temperature. Subsequently, the dried residue was heated in a quartz tube under a continuous stream of argon up to 550°C with 1 h isothermal hold Finally, the temperature was raised to 1000°C and held for 1 h The yield of the pyrolyzed powder was 75 g, i e., 81 wt% of the theoretical yield based on the polymethylsilazane-oxide-mixture used

In a subsequent step, the pyrolyzed powder was attritor milled in *n*-hexane for 3 h at 1000 rpm. The powder was then sieved in air with a 160 μm screen and subsequently cold-isostatically pressed at 630 MPa into green compacts of $35 \times 17 \times 15\,mm^3$ for the measurements of strength and fracture toughness, and into green compacts of 10 mm in length and 15 mm in diameter for the dilatometric measurements

In order to evaluate the results obtained from the polymer-derived material, we also prepared conventionally processed Si_3N_4/SiC specimens (reference samples) containing the same phase composition A mixture of commercially available powders, i e , 51 g α-Si_3N_4 (LC 10, H C. Starck, Berlin, Germany; which is converted to β-Si_3N_4 during the sintering

Table 1
Specific surface area, median particle size and analytical data of the polysilazane-derived and the conventionally processed powder systems after attritor milling for 3 h in *n*-hexane

Powder	*BET* (m^2/g)	d_{50} (μm)	*C* (*wt%*)	*N* (*wt%*)	*O* (*wt%*)	*Si* (*wt%*)
As-pyrolyzed[a] powder	—	—	12 6	26 8	0 5	58 9
Polymethylsilazane-derived powder[b]	17 2	0 72	9 7	19 4	14 2	—
Reference powder[c]	24 6	0 54	9 8	18 8	10 3	—

[a] Pyrolyzed at 1000°C in argon, material was not attritor milled
[b] Contains 85 wt% pyrolyzed polymethylsilazane, 10 5 wt% Al_2O_3 and 4 5 wt% Y_2O_3
[c] Contains 51 wt% α-Si_3N_4, 34 wt% β-SiC, 10 5 wt% Al_2O_3 and 4 5 wt% Y_2O_3

process), 34 g β-SiC (B 10, H C Starck, Berlin, Germany), 10 5 g Al_2O_3 and 4 5 g Y_2O_3 was attritor milled, dried, sieved and finally sintered just as in the processing as described above for the polymer-derived powder Table 1 summarizes the specific surface area, the median particle sizes and the analytical data obtained for both powder systems Particle size distributions of the attritor milled powders were determined by laser optical methods (Cilas HR 850 Granulometer, Alcatel, Marcoussis, France) Measurements of the carbon, nitrogen and oxygen content were performed by high temperature combustion methods (C, S Analyzer Model 244, N and O, Determinator Model TC 436, LECO Corp, St Joseph, MI, USA) Sintering experiments were conducted in a graphite resistively heated furnace (High-temperature furnace, Gero GmbH, Neuhausen, FRG) at 1750 and at 1850°C under 0 1 MPa N_2 Phase compositions were determined by X-ray diffraction (XRD) using monochromated $Cu_{K\alpha}$ radiation (wavelength 154 178 pm) Grain size distributions were obtained from SEM (Model S 200, Cambridge Instruments, Cambridge, UK)

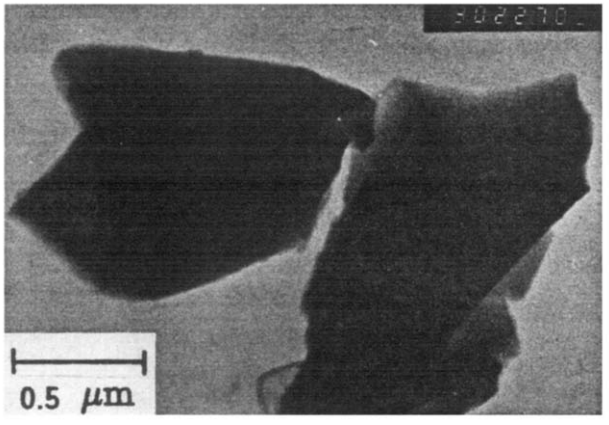

Fig. 1. TEM micrograph of polymethylsilazane pyrolyzed at 850°C for 1 5 h in argon

micrographs of etched surfaces Boiling (220°C) phosphoric acid (85%) was used as the etchant

Room temperature strengths, σ_B, were measured by four-point bending at a loading rate of 0 1 mm/min using polished rods of 25 × 2 5 × 3·0 mm^3 The critical stress intensity factor, K_{Ic}, was obtained by the indentation strength-in-bending test (ISB)[9] *E*-moduli were determined by the measurement of ultrasonic wave velocities The hardness was ascertained by the Vickers indentation method

3 Results and Discussion

3.1 Synthesis

Polymethylsilazane synthesized as reported by Seyferth and Wiseman[8] was pyrolyzed at 1000°C in an argon atmosphere giving a black, X-ray amorphous, silicon carbonitride (the presence of a silicon carbonitride is postulated due to ESCA measurements) as the residue with up to 85 wt% yield

$$[CH_3SiHNH]_{0.4}[CH_3SiN]_{0.6} \xrightarrow{1000°C} \text{'Si–C–N'} + CH_4 + H_2 + \quad (1)$$

During pyrolysis, the main decomposition of the polymethylsilazane occurred at 550°C with the simultaneous loss of methane and hydrogen as indicated in eqn (1)[8,10] Figure 1 shows a TEM micrograph of the material pyrolyzed at 850°C in argon indicating the amorphous state.

3.2 Analysis

If we use the chemical analysis of the pure as-pyrolyzed residue (see Table 1), a composition containing 67 wt% Si_3N_4, 27 wt% SiC and 4 wt% free carbon can be calculated by assuming all nitrogen atoms to be bonded to Si as Si_3N_4 and by assigning the residual Si atoms to SiC According to thermodynamic calculations, the excess carbon content will react with Si_3N_4 at temperatures above 1400°C in a nitrogen atmosphere (eqn (2))[11]

$$Si_3N_4 + 3C \xrightarrow{T \geq 1440°C} 3SiC + 2N_2 \quad (2)$$

Taking into account eqn (2), the weight ratio Si_3N_4 SiC is calculated to be 1 5 1 in polymethylsilazane-derived material heated at temperatures exceeding 1440°C. Thus, conventionally processed reference samples were prepared by mixing appropriate amounts of α-Si_3N_4 and β-SiC powders in the same calculated weight ratio. Additionally, 15 wt% oxide sintering additives (Al_2O_3 and Y_2O_3)[12] were added to both the polymer-derived and the reference powder as described earlier

The subsequent processing steps are summarized in Fig 2 The polymethylsilazane is dissolved in THF followed by suspension of the oxides After evaporation of the THF, the polymeric precursor is precipitated homogeneously on to the Al_2O_3 and Y_2O_3 particles The dried polymer-oxide mixture is then carefully pyrolyzed in argon up to 1000°C Prior to cold-isostatic pressing, the pyrolyzed residue has to be attritor milled in *n*-hexane in order to destroy the hard agglomerates developed during the heat-treatment Figure 3 represents the particle size distributions obtained from the different attritor milled powder systems

Due to the added 10 5 wt% Al_2O_3 and 4 5 wt% Y_2O_3, the theoretical oxygen content is calculated to be 5 9 wt% in both powder mixtures However, as can be seen in Table 1, the oxygen content in the reference powder has been determined to be 10 3 wt%, indicating additional hydrolysis of the Si_3N_4-particles during the milling process The oxygen content in the pyrolyzed and attritor milled polymer-derived powder has been found to be even higher (14 2 wt%) This increase of about 4 wt% is attributed mainly to a higher reactivity of the polymer-derived powder towards moisture as a consequence of its amorphous state. This high oxygen content is significantly reduced to 10 4 wt% (Table 2) after pressureless sintering of the powder at 1850°C in nitrogen atmosphere. Table 2 gives the C, N and O contents as analyzed for the sintered

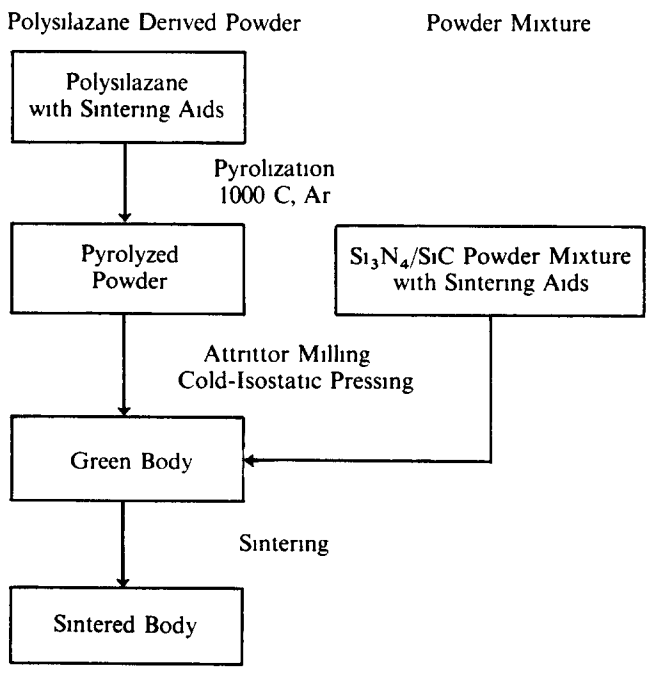

Fig. 2. Flow diagram of the processing procedure of the polysilazane-derived (left) and the conventionally mixed powders (right)

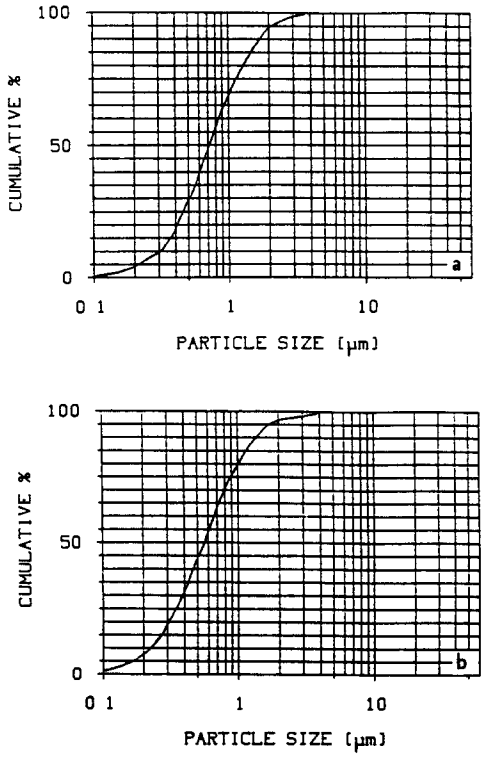

Fig. 3. Particle size distribution of the polysilazane-derived (a) and the conventionally mixed powder (b) both attritor milled in *n*-hexane for 3 h

amorphous powder as well as for the densified reference powder Comparing the analytical data of the polysilazane-derived powder (Table 1) with those of the sintered material (Table 2), a significant decrease of both oxygen and carbon and an increase of nitrogen is determined in the densified sample A Therefore, it is concluded that the excess carbon which is always present in the polymer-derived powder is consumed by reaction with silica during sintering according to eqns (3) and (4)

$$SiO_2 + C \xrightarrow{T \geq 1000°C} SiO + CO \quad (3)$$

$$SiO_2 + 3C \xrightarrow{T \geq 1000\ C} SiC + 2CO \quad (4)$$

It has been reported that the carbothermic reduction of silica may start even at temperatures between

Table 2
C, N and O contents measured in both the sintered polysilazane-derived material (sample A) and the sintered reference specimen (sample B)

Sample	*Powder source*[a]	*C* (*wt %*)	*N* (*wt %*)	*O* (*wt %*)
A	Polymethylsilazane-derived powder	7 1	22 5	10 4
B	Reference powder	9 0	20 6	9 2

[a] Powders cold-isostatically pressed at 630 MPa and sintered at 1850°C at 0 1 MPa nitrogen pressure

1000 and 1400°C depending mainly on the CO partial pressure [13] The commonly proposed reaction of carbon with Si_3N_4 according to eqn (2) obviously does not occur under these conditions

On the basis of the 7 wt% carbon measured in the sintered polysilazane-derived material (sample A, Table 2) the SiC content is calculated to be 24 wt% whereas the amount of SiC in the sintered reference specimen (sample B, Table 2) is determined to be 30 wt% (9 wt% carbon) Thus, despite the equal calculated phase compositions of both materials, sample A exhibits a 6 wt% lower SiC content than sample B The reason for this observed difference is attributable mainly to the individual sensitivity of both powders towards moisture Finally the presence of 20 wt% liquid phase is calculated for each of the sintered samples

3.3 Sintering

β-Si_3N_4 and β-SiC were detected as the crystalline phases in the densified (1850°C, 1 h) polymer-derived sample A by X-ray diffraction (Fig 4) The same phase composition was measured in the sintered reference sample B Figure 5 shows the sintering behaviour in a plot of the change in density versus temperature and time It is evident from Fig 5 that the polymer-derived powder starts from a relatively low green density of 1 49 g/cm^3 compared with a density of 1 99 g/cm^3 as determined for the green body of the reference sample Upon further heating at 20°C/min, the amorphous powder starts shrinkage at about 600°C The sintering rate is reduced in the temperature range between 1100 and 1450°C, probably due to the evolved gaseous CO generated by the reaction of carbon with silica as discussed above At temperatures between 1450° and 1750°C—where the liquid glassy phase containing

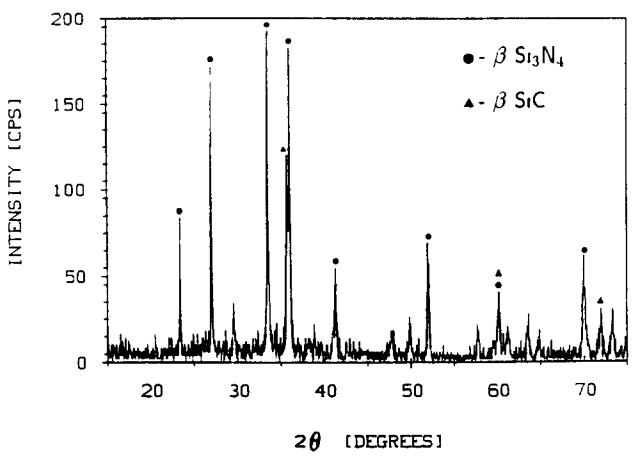

Fig 4 X-ray diffraction pattern of the polysilazane-derived powder sintered at 1850°C for 1 h in 0 1 MPa N_2 with an intermediate hold at 1750°C for 1 h

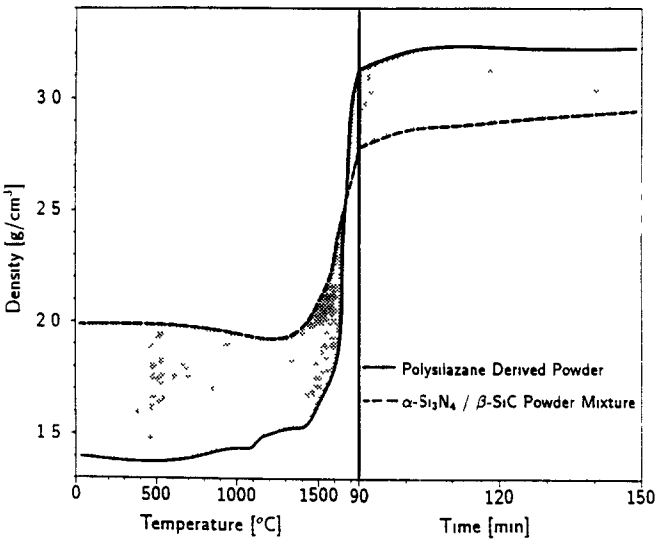

Fig. 5. Density change versus temperature and time of both polysilazane-derived and conventionally processed powder cold-isostatically pressed at 630 MPa Heating rate was 20 C/min The samples were isothermally held at 1750°C for 1 h

SiO_2, Al_2O_3 and Y_2O_3 is present—the polymer-derived powder shrinks with high sintering rates After 10 min isothermal hold at this last temperature, the material densifies to a final density of 3 23 g/cm^3, i e, 97% relative density assuming 3 33 g/cm^3 as the theoretical value Raising the temperature to 1850°C produces no further densification In contrast to the behaviour of the amorphous powder, the reference powder densifies with lower sintering rates between 1400 and 1750°C, and attains a density of 2 95 g/cm^3 (~89% relative density) during isothermal sintering at 1750°C for 1 h Further densification could be obtained by increasing the temperature to 1850°C for 1 h and the final density was determined to be 3 14 g/cm^3, i e, 94% relative density

The higher sinteractivity of the amorphous polymer-derived powder is explained by the interdependence of the densification rate and the grain size of the solid particles as commonly expressed in the equation developed for liquid phase sintering [14]

$$\frac{d\rho}{dt} = \frac{AD_l C \delta_l \Omega^2 \gamma_{l/s}}{G^4 RT} \tag{5}$$

where A is a geometrical constant, D_l the diffusion coefficient of the solved granular material in the liquid, C the solubility of the solid in the liquid, δ_l the thickness of the liquid film between the solid particles, Ω the atomic volume of the diffusing species, $\gamma_{l/s}$ the liquid/solid interfacial energy, G the grain size of the solid, T is temperature and t is time Due to the in-situ crystallization of the amorphous powder during sintering, nano-scale crystallites—

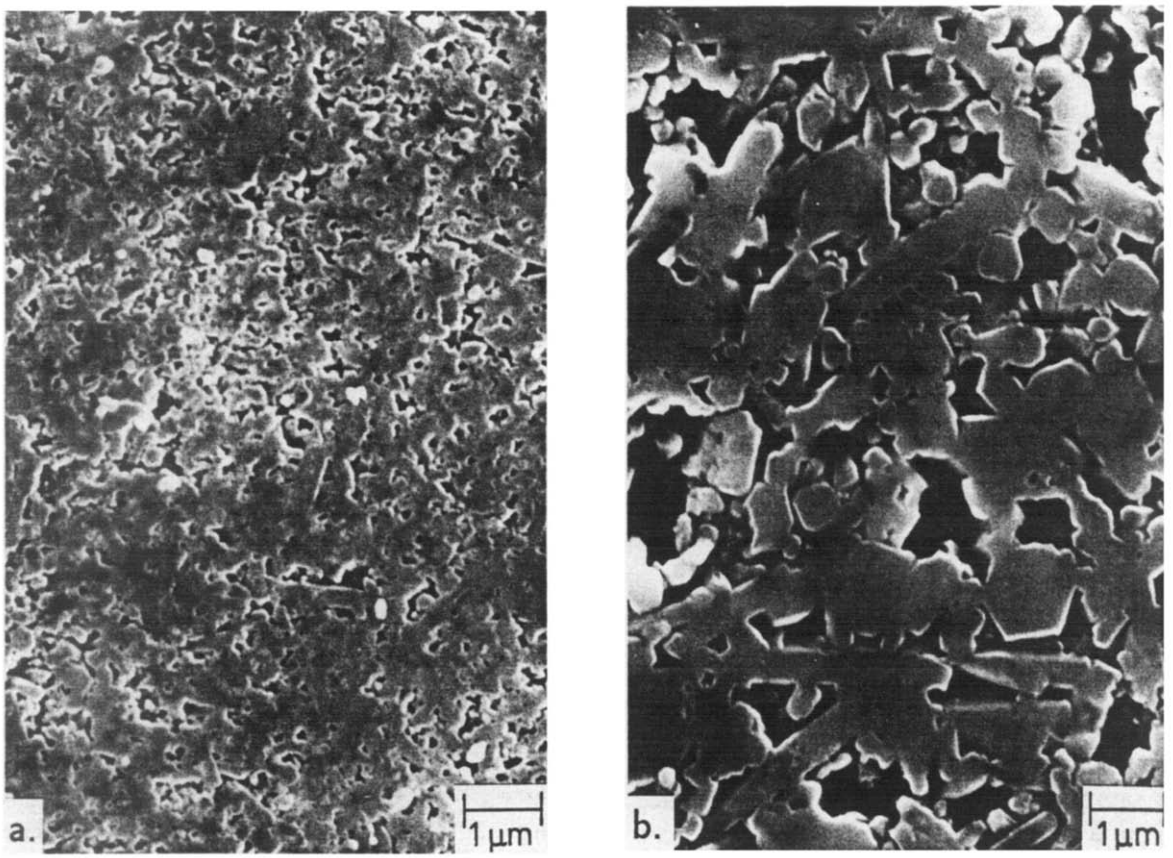

Fig. 6. SEM micrographs of etched surfaces of both the (a) sintered polysilazane-derived and (b) conventionally processed sample

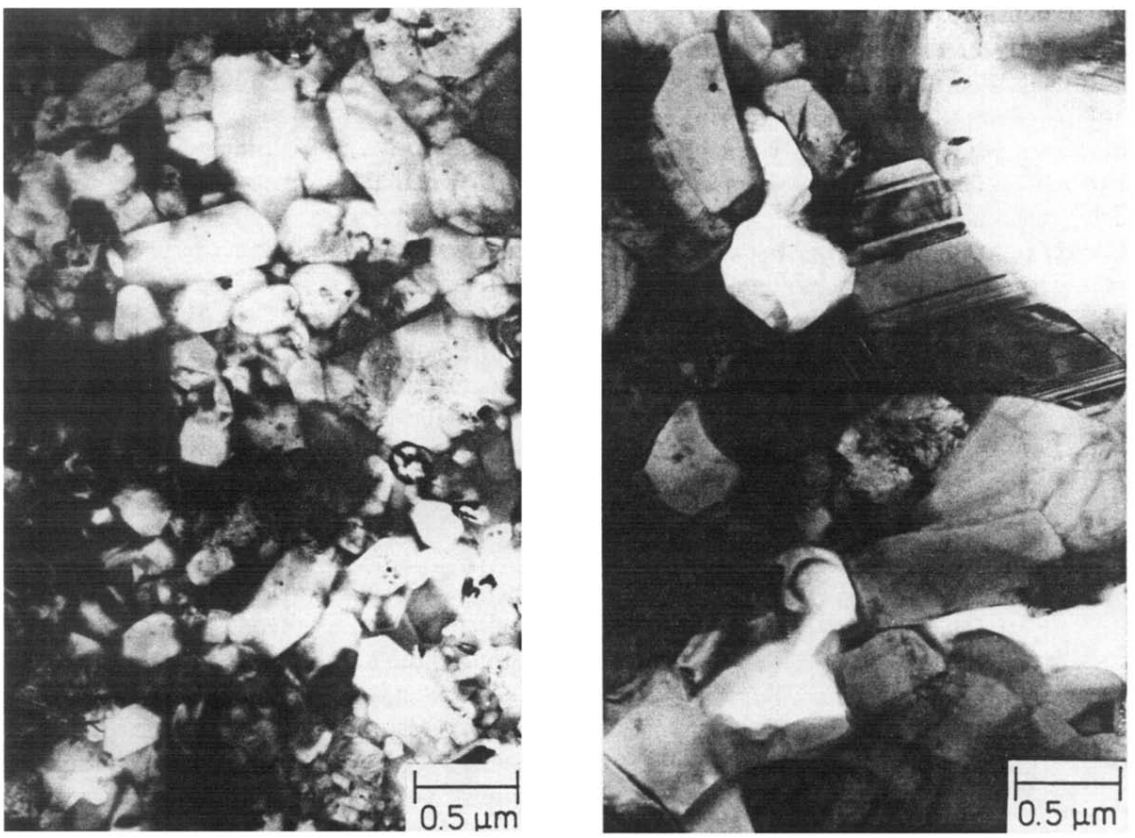

(a) (b)

Fig. 7. TEM micrographs of the (a) sintered polysilazane-derived and (b) conventionally processed sample

α-Si_3N_4 and β-SiC—are formed leading to the observed increase in the densification rate (eqn (5)), α-Si_3N_4 and β-SiC were detected as crystalline phases after heat-treatment of the amorphous material without any sintering additives at 1850°C in N_2 The polysilazane-derived powder can be sintered to full density even at 1750°C

3.4 Microstructure

The generated microstructures of the sintered specimens are represented in Figs 6 and 7 Figure 6 shows SEM micrographs of etched surfaces of both the polymer-derived material (Fig 6a) and of the conventionally processed sample (Fig 6b) The polymethylsilazane-derived sample exhibits a significant grain-refinement compared to the coarser microstructure developed on sintering of the commercial powder mixture The large voids observed in the microstructure of the reference sample B (Fig 6b) stem from glassy phase regions derived from the relatively inhomogeneously distributed oxide sintering additives and dissolved during the etching procedure Due to the smaller grains and hence the higher quantity of grain boundary surface, the regions of liquid phase segregation are much smaller in the polymer-derived microstructure of sample A Figure 7 shows additional TEM micrographs of both samples The phase distribution has also been measured by means of EELS in the TEM mode Thus, the crystallites exhibiting hexagonal symmetry could be identified as Si_3N_4 and the grains containing twins or stacking faults as SiC In addition to the presence of finer grains, a more homogeneous SiC distribution in the Si_3N_4-matrix can also be recognized in sample A

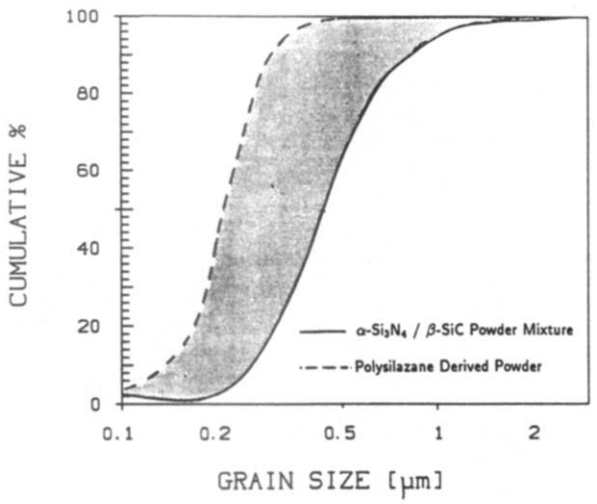

Fig. 8 Grain size distributions of the sintered (1850°C for 1 h in N_2) polysilazane-derived and conventionally processed sample

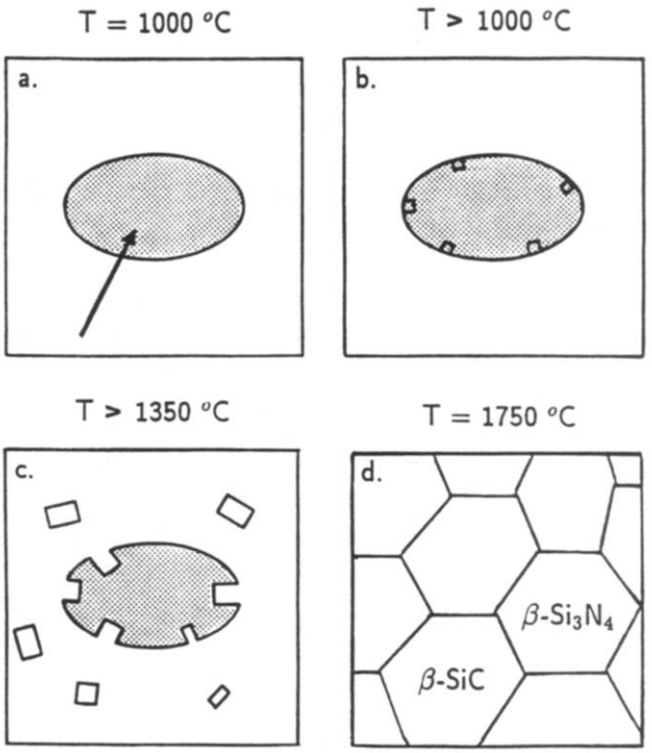

Fig 9. Schematic representing the proposed disintegration mechanism of the amorphous polymethylsilazane-derived powder occurring during sintering a = amorphous material at 1000 C, b = begin of crystallization (formation of α-Si_3N_4 and β-SiC), c = disintegration of the amorphous particle by removing of the generated crystallites by the liquid glassy phase, d = development of a homogeneous fine-grained β-Si_3N_4/β-SiC composite microstructure

A quantitative grain size distribution is given in Fig 8 which reflects the qualitative results based on the micrographs discussed above Lower median grain sizes ($d_{50} = 0\,2\,\mu m$) and a narrower grain size distribution ($d_{10} = 0\,13\,\mu m$, $d_{90} = 0\,28\,\mu m$) are determined in the polymer-derived sample A compared with the results obtained from the reference sample B ($d_{10} = 0\,25\,\mu m$, $d_{50} = 0\,4\,\mu m$, $d_{90} = 0\,8\,\mu m$)

The grain refinement observed in the polymer-derived sample is attributed to a particle disintegration process occurring during sintering.[15] Figure 9 shows a schematic of the proposed mechanism During the sintering process at 1000°C (Fig 9a) the silicon carbonitride powder is still amorphous Raising the temperature results in crystallization namely to α-Si_3N_4 and to β-SiC starting at the surface of the amorphous powder (Fig 9b) As soon as the first crystallites have been generated, grain boundaries are formed which will be wetted by the liquid glassy phase containing Al_2O_3, Y_2O_3 and SiO_2 at temperatures exceeding 1300°C Due to the wetting, the crystallites are removed from the amorphous solid by the liquid and

the amorphous particle subsequently disintegrates (Fig 9c) Generally, liquid phase sintering of the α-Si_3N_4 particles occurs via dissolution and reprecipitation in the form of β-Si_3N_4 [16,17] A similar solution-precipitation mechanism has been discussed for the sintering of SiC particles in this system [1] Since the in-situ generated crystallites are assumed to be extremely small—smaller than the particle size present in the attritor milled commercial powders as used in the reference sample B—the solubility in the glassy phase is enhanced yielding a highly supersaturated liquid Finally, the high supersaturation results in a high nucleation rate of β-Si_3N_4 and β-SiC nuclei and hence in the precipitation and formation of small β-Si_3N_4 and β-SiC crystallites giving the observed fine-grained microstructure (Fig 9d)

The discussed mechanism could be verified by the study of the crystallization behaviour of amorphous, polysilazane-derived silicon nitride powder (Fig 10) Therefore, amorphous Si_3N_4 was synthesized by pyrolyzing polymethylsilazane up to 1000°C in a continuous ammonia flow Optical transmission micrographs exhibit the amorphous state present in the colourless powder obtained at this temperature (Fig 10a) At higher temperatures (1300–1500°C), small crystallites are formed at the surface of the amorphous particles (Fig 10b) The crystallites indicated by arrows have been identified as α-Si_3N_4 by X-ray powder diffraction Finally, in order to observe the operation of the particle disintegration, amorphous Si_3N_4 powder with particle sizes greater than 32 μm —smaller particles were separated by sieving the powder through a 32 μm screen—has been annealed at 1700°C for 30 min in addition with 30 wt% glassy phase containing 37 wt% SiO_2, 24 wt% Al_2O_3 and 39 wt% Y_2O_3 (the composition represents a ternary eutecticum in the system Al_2O_3/SiO_2/Y_2O_3) [18] Figures 10c and d show optical micrographs of a polished surface of the slightly densified sample The dark particles consist of Si_3N_4 whereas the bright phase stems from the oxidic glass At this temperature (1700°C), it is obvious that the liquid glassy phase has penetrated into the former amorphous particles (arrow, Fig 10c) due to the wetting of the grain boundaries generated during crystallization Furthermore, some crystallites have

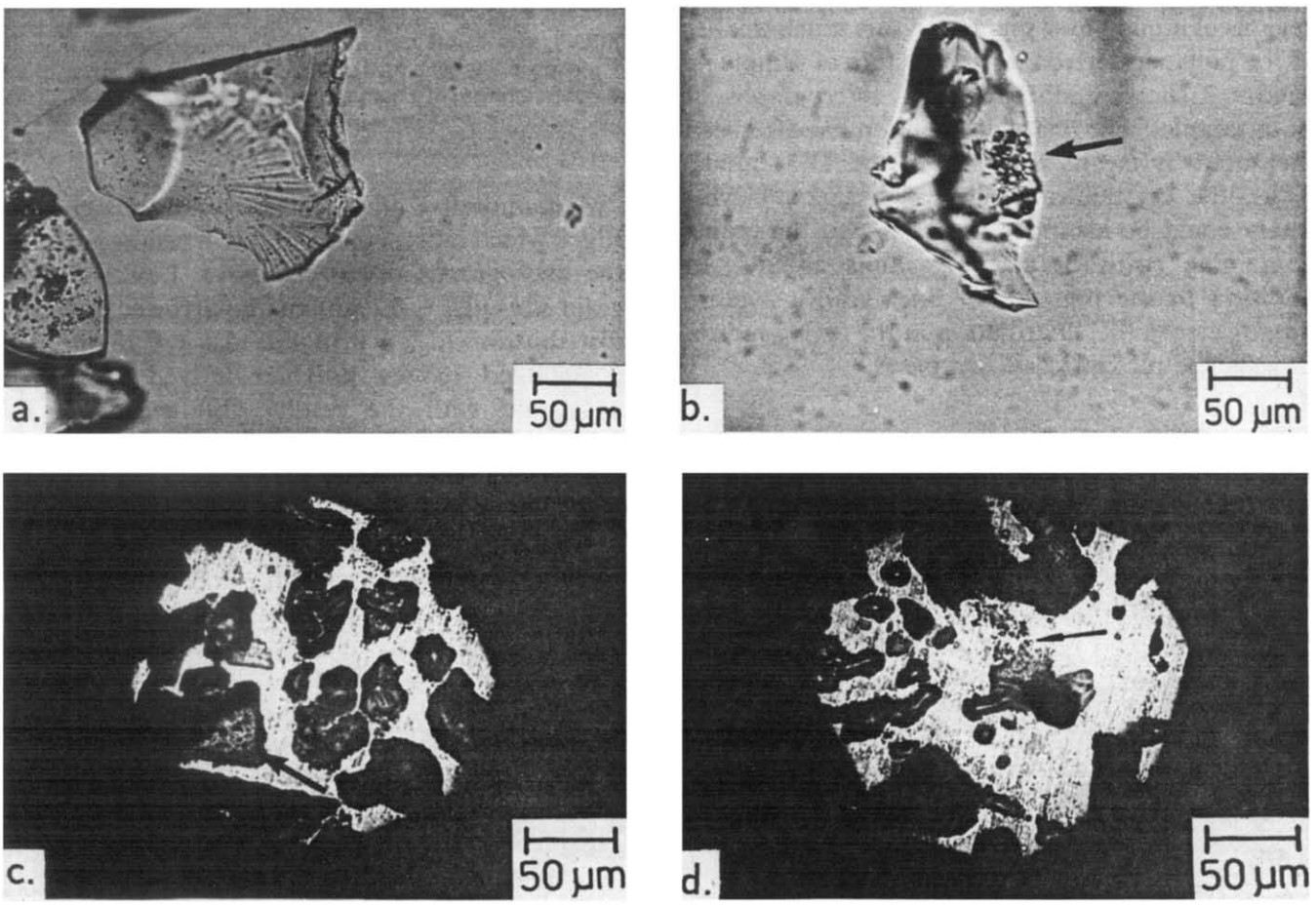

Fig. 10. Optical transmission micrograph of polymethylsilazane-derived amorphous Si_3N_4 powder pyrolyzed at 1000°C (a) under ammonia and (b) subsequently tempered at 1300°C, crystallites are marked with an arrow (c) and (d) show optical micrographs of amorphous Si_3N_4 powder annealed at 1700°C/30 min with 30 wt% glass phase (arrows see text)

Table 3
Mechanical properties of polysilazane-derived sample A and of conventionally processed sample B sintered at 1850°C in N_2 for 1 h

Property	*Sample A*	*Sample B*
Sinter density (g/cm^2)	3 15	3 08
Relative density (%)	95	93
Hardness HV10 (GPa)	14 5	11 3
E-Modulus (GPa)	286	251
K_{Ic} (MPa $\sqrt{m}$)	6 3	6 1
Flexural strength (MPa)	256 ± 17	228 ± 32
Median grain size (μm)	0 25	0 41
Median pore size (μm)	1 6	1 5

been disintegrated and can be found as small Si_3N_4 particulates ($\ll 32\ \mu$m) embedded in the glassy phase (arrow, Fig 10d)

3.5 Mechanical properties

Table 3 summarizes some mechanical properties as determined for the polysilazane-derived sample A, as well as for the reference specimen B The measured room temperature strengths, σ_B, of 256 and 228 MPa and fracture toughness values, K_{Ic}, of 6 3 and 6 1 MPa$\sqrt{m}$, respectively are similar to those reported in the literature [1] Whereas each of the samples, A and B, exhibits similar values for σ_B and K_{Ic}, it is important to note that the standard deviation of σ_B is significantly reduced in the specimen A The lower standard deviation indicates a better reproducibility of the properties and is to be understood in terms of the improved homogeneity of the polymer-derived microstructure (Figs 6 and 7)

Due to the smaller median grain size and the smaller grain size distribution of sample A, its fracture strength should be increased compared to that of sample B [19] That this is not the case, suggests that other strength limiting factors like pores, flaws or surface defects generated during the powder processing or grinding are still present

Furthermore, it is worth mentioning that the hardness as well as the Young's modulus has been determined to be higher in the polymer-derived material (Table 3)

Conclusion

Polymethylsilazane containing Al_2O_3 and Y_2O_3 could be converted into a sinteractive silicon carbonitride powder by pyrolysis at 1000°C in argon and by subsequent attritor milling of the residue The homogeneous distribution of the oxides is accomplished via a liquid phase precipitation of the polymeric precursor on to the oxide surfaces Thus, the amorphous polymer-derived powder could be pressureless sintered at 1750°C in nitrogen up to a final relative density of 97%, giving a Si_3N_4/24 wt% SiC composite The sintered samples exhibit a homogeneous distribution of the SiC particulates in the Si_3N_4-matrix The observed microstructure is characterized by relatively small grain sizes (d_{50} = 0 2 μm) and a narrow grain size distribution

The high sinteractivity, i e, the relatively low sintering temperature of 1750°C for full densification of the amorphous polymer-derived powder, is due to the nano-scale crystallites which are generated *in situ* during the sintering process, the observed fine-grained microstructure is attributed to a disintegration mechanism occurring in the amorphous material during sintering

The polysilazane-derived material exhibits room temperature strengths similar to those of conventionally processed samples However, the standard deviation of σ_B is significantly reduced in the polymer-derived sample indicating an improvement in the reproducibility of the mechanical properties due to the homogeneous distribution of the dispersed composite phases and of such faults as flaws or pores developed during the powder processing and sintering step

Acknowledgements

The authors wish to thank Prof R J Brook for fruitful discussions and W Szabo for the TEM microscopy Dr M Peuckert, Dr H -J Kleiner and Dr T Vaas, Hoechst AG, Frankfurt, are acknowledged for the preparation and provision of the polymethylsilazane

References

1 Greil, P , Petzow, G & Tanaka, H , Sintering and hipping of silicon nitride–silicon carbide composite materials *Ceram Int*, **13** (1987) 19
2 Weiser, M W & De Jonghe, L C , Inclusion size and sintering of composite powders *J Am Ceram Soc*, **71**(3) (1988) C-125
3 Raj, R & Bordia, R K Sintering behaviour of bi-modal powder compacts *Acta Met*, **32** (1984) 1003
4 Bordia, R K & Raj, R , Hot isostatic pressing of ceramic/ceramic composites at pressures ≤ 10 MPa *Adv Ceram Mat*, **3**(2) (1988) 122
5 Lange, F F , Effect of microstructure on the strength of Si_3N_4–SiC composite systems *J Am Ceram Soc*, **56** (1973) 445
6 Riedel, R , Strecker, K & Petzow, G , In-situ polysilane-derived SiC particulates dispersed in Si_3N_4 composite *J Am Ceram Soc*, (in press)

7 Sawhill, H T & Haggerty, J S, Crystallization of ultrafine amorphous Si_3N_4 during sintering *J Am Ceram Soc*, **65** (1982) C-131
8 Seyferth, D & Wiseman, G, High-yield synthesis of Si_3N_4/SiC ceramic material by pyrolysis of a novel polyorganosilazane *J Am Ceram Soc*, **67** (1984) C-132
9 Anstis, G R, Chantikul, P, Lawn, B R & Marshall, D B, A critical evaluation of indentation techniques for measuring fracture toughness I, Direct crack measurements *J Am Ceram Soc*, **64** (1981) 533
10 Seher, M, Herstellung von Si_3N_4/SiC Composit-Keramiken aus polymeren Vorstufen Diplomarbeit, Universitat Stuttgart, FRG, 1989
11 Nickel, K G, Hoffmann, M J, Greil, P & Petzow, G, Thermodynamic calculations for the formation of SiC-whisker-reinforced Si_3N_4 ceramics *Adv Ceram Mat*, **3**(6) (1988) 557
12 Omori, M & Takei, M, Pressureless sintering of SiC *J Am Ceram Soc*, **65** (1982) C-92
13 Jong, B W, Formation of silicon carbide from silica residues and carbon *Am Ceram Soc Bull*, **58** (1979) 788
14 Salmang, H & Scholze, H, *Keramik, Teil 1 Allgemeine Grundlagen und wichtige Eigenschaften* 6 *Auflage*, Springer Verlag, Berlin, 1982, p 181
15 Kaysser, W A, Liquid phase sintering of composites In *Processing and Properties for Powder Metallurgy Composites*, ed P Kumar, K Vedula & A Ritter The Metallurgical Society, Warrendale, PA, 1988, pp 21–43
16 Ziegler, G, Heinrich, J & Wotting, G, Relationships between processing, microstructure and properties of dense and reaction-bonded silicon nitride *J Mat Sci*, **22** (1987) 3041
17 Kingery, W D, Densification during sintering in the presence of a liquid phase I Theory *J Appl Phys*, **30** (1959) 301
18 Bondar, I A & Galakhov, F Izv Akad Nauk SSSR, *Ser Khim*, **7** (1963) 1325
19 Knudsen, F P, Dependence of mechanical strength of brittle polycrystalline specimens on porosity and grain size, *J Am Ceram Soc*, **42** (1959) 376